Identification of the transition state for fast reactions: The trapping of hydroxyl and methyl radicals by DMPO—A DFT approach

Benjamín Aguilera-Venegas [a,b,*], Hernán Speisky [a,c]

[a] Laboratory of Antioxidants, Institute of Nutrition and Food Technology, University of Chile, Av. Macul 5540, P.O. Box 138-11, Santiago, Chile
[b] Department of Inorganic and Analytical Chemistry, University of Chile, Box 233, Santiago, Chile
[c] Department of Chemical Pharmacology and Toxicology, Faculty of Chemical and Pharmaceutical Sciences, University of Chile, Box 233, Santiago, Chile

ABSTRACT

Up to date, attempts to locate the transition state (TS) for the trapping reaction between $^\bullet$OH and DMPO have been unsuccessful, and the lack of molecular mechanisms by which $^\bullet$OH binds to the spin-trap constitutes a question still unsolved. Herein, we have taken a step forward on this task by describing the theoretical TS for the trapping of $^\bullet$OH and $^\bullet$CH$_3$ by DMPO and the intrinsic reaction coordinates. This work aims to provide new understandings on the molecular orbital (MO) interactions that rule these reaction paths. Besides we assessed the degree of involvement of weak interactions and the charge transfer (CT) phenomenon involved in such interactions. Regarding the trapping of $^\bullet$OH, the beginning of the reaction would be ruled by weak interactions to then give way to stronger MO interactions conducive to the formation of the TS. For $^\bullet$CH$_3$, the reaction is, instead, early ruled by significant MO interactions, and a relatively small contribution in the weak interactions range. At the TS, both reactions share the formation of an antibonding orbital responsible for hosting the unpaired electron, and two bonding orbitals between the radical and the spin-trap. Additionally, the charge is transferred primarily from DMPO to $^\bullet$OH through β orbitals, while for $^\bullet$CH$_3$, the CT occurs in both directions, so that while DMPO behaves like an α-acceptor/β-donor, $^\bullet$CH$_3$ acts as a β-acceptor/α-donor. Finally, we provide evidence showing that the resultant theoretical models are in agreement with the hyperfine coupling constants as obtained from biological-ESR spin trapping experiments.

© 2014 Elsevier Inc. All rights reserved.

1. Introduction

The continuous disruption of redox signaling processes by free radicals often leads to uncontrolled alterations in the redox status of cells which, ultimately, either trigger and/or accelerate the development of a various oxidation-related human pathologies (e.g. some tumoral, cardiovascular and neurodegenerative diseases). Oxidative alterations, however, can also become a pharmacological tool for the treatment of certain pathologies, such as it occurs in parasitic diseases, and certain forms of cancers [1,2]. Consequently, the accurate detection and quantification of free radicals in biological systems is a relevant issue in the search of new targeted drugs. There are several ways to assess the progress of the free radicals production along a biological reaction. One of them, is by means of ESR-based techniques which, besides providing an overview about the production of free radicals, allows the identification of very short-lived radicals (e.g. $^\bullet$OH, O$_2$$^{\bullet-}$) by means of their characteristic and easily recognizable ESR spectrum and hyperfine coupling constants (HFCCs). In the spin-trapping technique, a spin-trap molecule reacts with a short-lived radical leading to the formation of a spin-adduct, a "more stable radical" which exhibits a longer half-life than the isolated radical [3]. Thus, the spin-trapping technique offers a practical form to establish what kind of radical can be generated by recently synthesized ROS-producing drugs [4]. However, whenever the HFCCs are the only parameters under determination, the electronic/molecular structures of the spin-adduct cannot be categorically established [5], and therefore, an interpretation solely based on HFCCs data can eventually lead to misleading conclusions [6].

Up to date, a variety of spin-trapping reactions have been theoretically addressed. Among these are the reactions between methyl, superoxide, hydroxyl, hydroperoxy and nitric oxide radicals alongside several spin-traps [7–10]. Most studies conducted so far have focused their attention on discussing prediction of thermodynamic parameters, decay pathways, and rate constants [11]. However, the process by which the radical and the spin-trap interact to give rise

* Corresponding author at: Laboratory of Antioxidants, Institute of Nutrition and Food Technology, University of Chile, Av. Macul 5540, P.O. Box 138-11, Santiago, Chile. Tel.: +56 2 29782963; fax: +56 2 27370567.

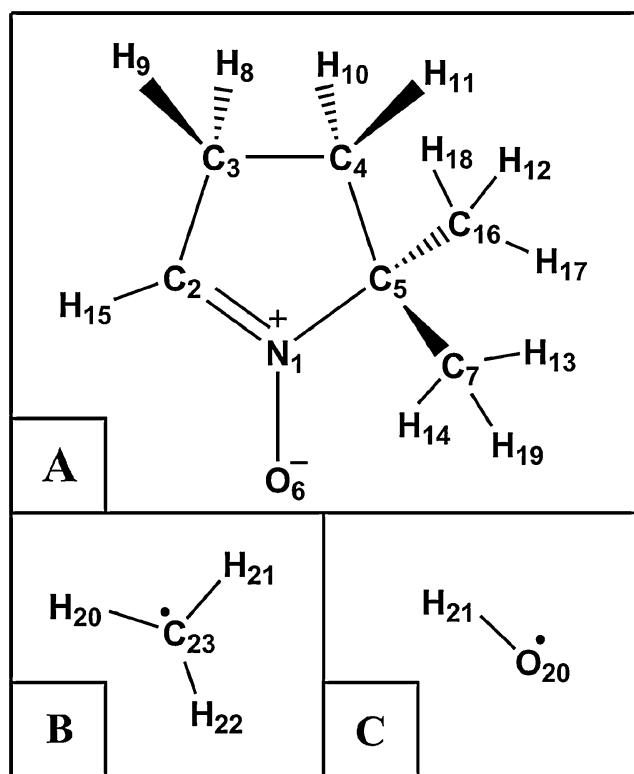*E-mail address:* benya@ciq.uchile.cl (B. Aguilera-Venegas).

Fig. 1. Arbitrary numbering of the atoms involved in the reactions here investigated. (A) DMPO, (B) methyl radical and (C) hydroxyl radical.

to a binding interaction constitutes a largely unsolved issue. In fact, attempts to locate the transition state (TS) for the trapping reaction between •OH and DMPO (5,5-dimethyl-1-pyrroline-*N*-oxide) have been unsuccessful, thus leaving a void in current knowledge on this type of reactions, so far, limited to the understanding of the independent states, i.e. reactants and products [9]. Thus, in order to fill the above-referred void, the present work aims to provide an accurate picture of the entrapment reactions between some biologically relevant radicals (•OH and •CH₃) and DMPO (Fig. 1).

These radicals were chosen mainly due to their biological implications. Thus, •OH is one of the main radicals involved in diseases and metabolism, while •CH₃ may be released through different paths derived from reactions wherein •OH is involved [12]. In order to gain insight into the molecular orbital reactivity, this study was carried out chiefly through energy and charge decomposition analysis. Afterwards, in order to find out if there is any additional factor capable of affecting the reaction pathways, non-covalent interactions were analyzed by the reduced density gradient (RDG) method [13], derived from AIM analysis [14], which results reliable for both simple and complex systems containing either a few, or many atoms [15]. Thus, in order to rationalize the resulting theoretical models, the usual magnitude of the hyperfine coupling constants obtained from spin-trapping experiments were taken from previous reports (or spin-trap databases) and compared with our theoretical results.

2. Methodologies

2.1. Theoretical procedures

Unless indicated otherwise, the standard procedures were as follows: the initial structural models for reactants and products were built with Spartan 10 [16]. Minimum energy conformers were located by MMFF and optimized later with semiempirical (AM1)

methods. All following calculations were performed with Gaussian 09 [16]. Resultants geometries were re-optimized by AM1 at a full convergence criterion (very tight). The first guesstimate to the transition state (TS) was performed with QST2 [17] at AM1 level, and the intrinsic reaction coordinate (IRC) was estimated later at the same theory level. Afterwards, starting from the IRC results the resultant structures for reactants and products were taken (also optimized as described above) and used as initial guess for a QST3 calculation at AM1 level again (the initial guess for the TS structure corresponded to that of the QST2 calculation) and the IRC was calculated. Each TS structure was confirmed and characterized by a single negative (imaginary) frequency. The frequencies for all stationary points are available as supplementary information (**SI**)†.

Afterwards, starting from the QST3 calculation results (at AM1 level), the structures for reactants and products were taken and subsequently used as guess structures for high theory-level calculations. Final TS and IRC calculations were performed with QST2 (or QST3) at (U)B3LYP/6-31G(d) level [18,19], and the reactants (and products) were re-optimized at the referred level. Additionally, solvation effects were included in calculations for TS, IRC, reactants and products by the continuous surface charge polarizable continuum model [20]. The optimized geometries resulted in complete agreement with the available X-ray crystallography data for the bond lengths N1 = C2, N1–O6 (as spin-trap), N1–C2 and N1–O6 (as spin-adduct) [21–23]. The optimized geometries are available as supplementary information (**SI**)†. Single point calculations for spin-adducts were performed at (U)B3LYP/6-31G(d) [24] level together with the aforementioned solvation model previously described as a proper model to estimate the hyperfine interactions [25].

Mulliken population analysis (MPA), energy decomposition analysis (EDA) [26,27], charge decomposition analysis (CDA) [28,29] (as well as its extended version ECDA) [30,31], orbital interaction diagrams, and partial/total density of states plots were performed with AOMix [32]. Total and partial density of states plots are scaled by 1/2. Fragments for population analysis were partitioned in terms of the Dewar-Chatt-Duncanson model. Atomic charges and spin densities were calculated at (U)B3LYP/6-31G(d) (PCM) level under MPA and NPA [33] (implemented by NBO5.G [34]) partition models. Analysis of the wavefunction such as RDG [13], AIM [14] and CT analysis based on the Le Bahers' method [35] were performed with Multiwfn [36]. Isosurfaces were built with Avogadro [37] or VMD [38], and traced with POV-Ray [39]. Details about acronyms and abbreviations are summarized in supplementary information (**SI**)†.

3. Results

3.1. REACTION 1: DMPO + •OH → •DMPO-OH

3.1.1. Intrinsic reaction coordinate

The reaction pathway for the entrapment reaction between the hydroxyl radical and DMPO (Fig. 2) begins by reducing the distance between O20 and C2 in parallel to the variation of the dihedral angle formed by C2–C3–C4–H10 in such way that this angle varies drastically from 143.05° to 97.83° what makes that C2 gets closer to O20 shortening its distance from 3.5 Å to 2.2 Å. Subsequently, the distance between H21 and O6 is slightly increased until DMPO reaches a flat conformation with an angle close to zero for the dihedral C2–C3–C4–C5. After that, the distance H21···O6 is further increased (~0.75 Å), and the H15 (partially) gets out of the ring plane, thus reaching the transition state. In the downhill of the reaction pathway, the distance O20···C2 is shortened until 1.4 Å whereas the C2–N1 bond is lengthened in 0.11 Å, thus leading to the formation of the single bond O20–C2. In parallel to the above, to the extent to which C2 gets closer to O20 (mainly through the